Science of the Total Environment 954 (2024) 176196

Contents lists available at ScienceDirect

Science of the Total Environment

journal homepage: www.elsevier.com/locate/scitotenv

Modeling bacterial transport and fate: Insight into the cascading consequences of soil water repellency and contrasting hydraulic conditions

Nasrollah Sepehrnia [a,b,*], Forough Abbasi Teshnizi [c], Paul Hallett [a], Mark Coyne [d], Nima Shokri [e,f], Stephan Peth [g]

[a] School of Biological Sciences, University of Aberdeen, Aberdeen, UK
[b] School of Biosciences, University of Nottingham, Nottingham, UK
[c] Department of Water Engineering, Faculty of Agriculture, Shahrekord University, Shahrekord, Iran
[d] University of Kentucky, Department of Plant and Soil Sciences, United States[1]
[e] Institute of Geo-Hydroinformatics, Hamburg University of Technology, Am Schwarzenberg-Campus 3 (E), 21073 Hamburg, Germany
[f] United Nations University Hub on Engineering to Face Climate Change at the Hamburg University of Technology, United Nations University Institute for Water, Environment and Health (UNU-INWEH), Hamburg, Germany
[g] Institute of Earth System Sciences, Leibniz Universität Hannover, Herrenhäuser Str. 2, D-30419 Hannover, Germany

HIGHLIGHTS

- Modeling showed bacteria attached to natural soils rather than undergoing significant straining.
- Greater bacteria attachment occurred in wettable soil than water-repellent soil.
- Water-repellency caused selective bacteria physical release or physicochemical detachment.
- Optimizations showed small hydrophobic *Rhodococcus erythropolis* detached, large hydrophilic *Escherichia coli* released.
- Separate optimization of bacteria pulses highlighted physical straining and release roles.

GRAPHICAL ABSTRACT

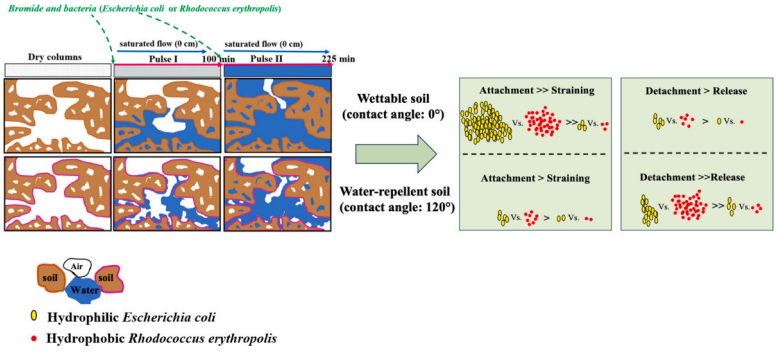

ARTICLE INFO

Editor: Deyi Hou

Keywords:
Bacteria
Attachment
Wettability
Water repellency
Straining
Transport processes

ABSTRACT

The mechanisms governing bacteria transport and fate rely on their hydrophobicity and the wettability of porous media across a wide range of soil moisture conditions, extending from extreme dryness to highly saturated states. However, it largely remains unknown how transport, retention, and release mechanisms change in natural soil systems in such conditions. We thus optimized our previously published unique transport data for hydrophilic *Escherichia coli* (*E. coli*) and hydrophobic *Rhodococcus erythropolis* (*R. erythropolis*) bacteria, and bromide (Br^-) in two distinct wettable and water-repellent soils at column scale. The soils were initially dry, followed by injecting influents in two pulses followed by a flushing step under saturated flow conditions for six pore volumes. We conducted simulations for each pulse separately and simultaneously for soils. There were differences in hydraulic properties of the soils due to their contrasting wetting characteristic in separate and simultaneously modeling of

* Corresponding author at: School of Biological Sciences, University of Aberdeen, Aberdeen, UK.
E-mail address: nasrollah.sepehrnia@abdn.ac.uk (N. Sepehrnia).
[1] (emeritus).

https://doi.org/10.1016/j.scitotenv.2024.176196
Received 6 May 2024; Received in revised form 2 September 2024; Accepted 9 September 2024
Available online 13 September 2024

each pulse affecting Br^- and bacteria transport fate. Bacteria attachment was the dominant retention mechanism in both soils in these conditions. Notably, the 82.4 min^{-1} attachment rate in wettable soil was almost 10× greater than in the water-repellent soil and it governed optimization of bacteria die-off. Physicochemical detachment and physical release unraveled the effect of bacteria size and hydrophobicity interacting with soil wettability. The smaller and hydrophobic *R. erythropolis* detached more easily while hydrophilic *E. coli* released; the rates were enhanced by soil water repellency. Further research is needed to reveal the effects of surface wettability properties on bacteria survival especially at the nanoscale.

1. Introduction

Climate change and global warming associated with rising temperatures, declining rainfall or erratically distributed precipitation have led to increased drought conditions that alter soil properties (Bachmann et al., 2021; Sepehrnia and Bachmann, 2022). On drying, wettable soils can change to water-repellent soils due to presence of hydrophobic materials (e.g., mainly originated from organic matters), resulting in increased runoff, groundwater contamination, accelerated soil erosion, and adverse effects on agricultural production (Hewelke et al., 2022; Sepehrnia et al., 2018b). These unexpected meteorological and hydrological events undoubtedly affect the colonization, survival, and persistence of bacteria - including pathogens - in soil and water bodies (Hellberg and Chu, 2016). The fate of bacteria thus depends on a range of physical, chemical, biological, and hydrological conditions in the soil (Bai et al., 2016, 2017, 2023).

Soil water repellency (SWR) affects accessibility and attachment of bacteria to soil particle surfaces, due to localized flow rates, patchy wetting, and interfacial interactions between water and soil particles (Goebel et al., 2013; Goebel et al., 2011; Sepehrnia et al., 2019; Sepehrnia et al., 2018b). Soil water repellency reduces the water film thickness on particles, restricting access by microbes and plant roots to water and nutrients. This affects biological activities and the fate of bacteria (Braun et al., 2010; Goebel et al., 2013; Goebel et al., 2011). The alterations in the bio-physicochemical features of soil due to SWR can affect bacterial transport, a critical factor in soil and water contamination (Sepehrnia et al., 2023; Sepehrnia et al., 2018a). Soil water repellency has a significant effect on water flow and can change transient water content (Bachmann et al., 2007). This can release attached or strained bacteria from film water and immobile water zones due to sudden shifts in soil water content, water saturation, and water film thickness temporally and spatially (Sepehrnia et al., 2023; Sepehrnia et al., 2018b).

Clay content also plays a crucial role in the interactions between microorganisms and soil due to its active physical and chemical properties, such as high adsorptive capacity, surface area, structure, water retention, and cation exchange capacity (Fomina and Skorochod, 2020). These properties, combined with bacterial properties, can be driving factors influencing bacteria attachment and detachment and hence mobility, especially when soils are dry. For instance, *Pseudomonas putida* attaches to the clay fraction 4 and 62 times more than the silt and sand fractions, respectively (Wu et al., 2011). Other research finds that positively charged pyrophyllite clay, compared to neutral sand materials, has an effective role in removing negatively charged *E. coli* due to the attachment of the bacteria (Kang et al., 2013).

Survival is a further important factor affecting bacteria transport and fate. The mortality of bacteria and pathogens in soil is crucial to environmental health, soil health, and ecosystem function, making it useful to understand and manage bacterial die-off and survival. Variations in soil conditions and moisture levels significantly influence bacterial survival rates and community dynamics (Rodrigues and de Carvalho, 2019). For instance, the attachment of bacteria to soil particles helps maintain their viability and reduce mortality rates, as particle-attached bacteria generally exhibit lower decay rates than their free-living counterparts (Nakhle et al., 2021). Moisture retention, influenced by particle size distribution and organic matter content, emerges as a particularly significant factor affecting bacterial persistence fate (Alegbeleye and Sant'Ana, 2023). Wang et al. (2023) noted that osmotic pressure differences can lead to cell dehydration, membrane damage, and protein denaturation, ultimately resulting in the death of *E. coli*. Wang et al. (2023) noted that soil texture and temperature are vital for bacterial survival and persistence. Similarly, Ghosh (2023) found that soil texture and macronutrients significantly affect *E. coli* survival in agricultural soils, with *E. coli* showing greater survival rates in clay loam than silt loam soil under nutrient-free conditions. Limoges et al. (2022) further demonstrated that nitrogen availability, especially in organic forms like urea and protein, is crucial for *E. coli* survival in nutrient-rich environments. The attachment and thus survival of bacteria to soil surfaces (considering their cell hydrophobicity and surface macromolecules such as flagella) from very dry to moist conditions, can intricately influence subsequent transport and retention (Sepehrnia et al., 2018a, 2019, 2023).

The subject of bacteria transport has received much attention in unsaturated and saturated conditions either through experimental or modeling studies (e.g., 40–100 % degree of saturation (Bradford et al., 2015; Bradford et al., 2013; Sepehrnia et al., 2014; Torkzaban et al., 2007). However, modeling data with regards to extremely low soil moisture, particularly with respect to inherent soil properties such as clay, silt, and sand contents and water repellency, has received less attention in naturally wettable and water-repellent soils (Sepehrnia et al., 2018a, b). It is commonly accepted that in dry conditions, most soils exhibit some level of water repellency (Bachmann et al., 2021).

Systematic modeling studies using HYDRUS software in clean bed porous media demonstrate the responses of wettable and water-repellent sandy media for retaining bacteria from an initially dry soil condition through to rewetting up to saturation (Sepehrnia et al., 2023; Sepehrnia et al., 2018a). However, a knowledge gap remains for naturally wettable and water-repellent soils which is addressed in this paper. By extension, it is not clear how bacteria transport, retention and release mechanisms change in natural soil systems under contrasting hydraulic conditions ranging from extremely dry to very wet in the presence of water repellency. Therefore, the main aims of this study were: i) to determine the dominant mechanisms of bacterial transport and retention through dry wettable and water-repellent soils; ii) to evaluate the performance of HYDRUS in predicting bacteria fate to distinguish the magnitude of bacteria attachment and straining with regard to abrupt changes in soil wettability.

2. Material and methods

The main experimental measurements and data are presented in Sepehrnia et al. (2019) and the focus of the current study is to model bacteria transport and fate using those experimental data. Notwithstanding, for better illustration, we have summarized them as follows.

2.1. Bacteria and soil characterization

Suspensions of *E. coli* (hydrophilic, 2.05 μm) and *R. erythropolis* (hydrophobic, 1.47 μm) at 1.00×10^8 CFU mL^{-1} were prepared with pH of 7.10 and electrical conductivity of 1.41 dS m^{-1}.

2.2. Soil columns

Wettable and water-repellent Haplic Cambisols (IUSS Working Group WRB, 2022) were collected from a pasture in Shahrekord (32° 19' 16" N, 50° 46' 26" E), Iran. The wettable soil had a contact angle of 0°, while the water-repellent soil had a contact angle of 120°. Soil samples were characterized for texture, organic carbon, EC, pH, and cation exchange capacity (CEC) using routine procedures (Table 1). The wettable soil had greater sand and silt content than the water-repellent soil, but less clay, OC, and CEC (Table 1). Soil columns (18.2 cm height, 7 cm diameter) were prepared by uniformly packing the soils to field bulk densities of 1.2 g cm^{-3} (wettable) and 0.94 g cm^{-3} (water-repellent) with porosities of 0.53 (±0.12) and 0.55 (±0.10), respectively. Parameterization of soil hydraulic properties data given by Sepehrnia et al. (2019) was performed according to Durner's bimodal hydraulic model (Durner, 1994) (Table 2).

2.3. Leaching experiments

Leaching experiments involved two pulses (I and II) of bacterial suspensions and bromide (Br^-) injected into soil columns. The injection of two influent pulses was to differentiate the main mechanisms of bacteria transport, retention, and release under contrasting hydraulic conditions. The first pulse included 1.00×10^8 CFU mL^{-1} bacteria and 10 mM Br^- under saturated flow, with effluents collected to analyse bacterial and Br^- concentrations. The second pulse followed with identical concentrations, continuing leaching for six pore volumes. Bacterial concentrations were determined via plate-counting on selective media (Guber et al., 2007), and Br^- concentrations were measured using an ion-selective electrode (Sepehrnia et al., 2018b). The experimental breakthrough curves data (from Sepehrnia et al. (2019)) are shown by symbols in Figs. 1–4.

2.4. Mathematical modeling of bacteria and bromide transport

Extending from Sepehrnia et al. (2019), we conducted simulations of the transport of bromide and bacteria in two stages: (i) simultaneous simulation of two pulses together; (ii) separate predictions for dry and wet pulses. For Br^-, inverse optimizations were performed using the Mobile Immobile Model (MIM) with non-equilibrium physical condition for solute transport (Eqs. 1 and 2, e.g., Šimůnek and van Genuchten, 2008; Šimůnek et al., 2003) implemented in HYDRUS-1D (version 4.16.0110) (PC Progress, Riverside, USA). The experimental data were optimized to simulate Br^- dispersivity (λ), saturated and immobile water contents (θ_s and θ_{im}), saturated hydraulic conductivity (K_s), and mass transfer coefficient for Br^- exchange between mobile and immobile liquid regions (α). Bromide was not excluded from the immobile regions due to the dynamics of sand wettability and the initial dry conditions of the columns and thus the exchange of Br^- between the mobile and immobile regions ($\alpha \neq 0$).

$$\theta_m \frac{\partial C_m}{\partial t} + \theta_{im} \frac{\partial C_{im}}{\partial t} = \theta_m D_m \left(\frac{\partial^2 C}{\partial x^2} \right) - \theta_m v_m \frac{\partial C_m}{\partial x} \quad (1)$$

$$\theta_{im} \frac{\partial C_{im}}{\partial t} = \alpha (C_m - C_{im}) \quad (2)$$

where C is Br^- concentration in the soil solution [M L^{-3}], t is time [T], ν is pore water velocity [L T^{-1}], D is dispersion coefficient [L^2 T^{-1}] yielded from dispersivity (λ, [L]) and apparent pore water velocity ($D = \lambda\nu$) [LT^{-1}]. Subscriptions m and im refer to mobile and immobile water regions. The predicted hydraulic characteristics were used to optimize bacteria transport, retention, and release mechanisms. The Two Kinetics Sites model (Eq. 3) was applied using HYDRUS-1D to model the process (Šimůnek and van Genuchten, 2008).

$$\theta \frac{\partial C}{\partial t} + \rho_b \frac{\partial S_1}{\partial t} + \rho_b \frac{\partial S_2}{\partial t} = \lambda \theta v \frac{\partial^2 C}{\partial x^2} - \theta v \frac{\partial C}{\partial x} \quad (3)$$

where C [N_c L^{-3}] is the bacteria concentration in the aqueous phase, where N_c is the number of colloids), S is the soil mass related concentration of attached bacteria [N_c M^{-1}], ρ_b is the bulk density of the soil [M L^{-3}], x is the distance in the vertical direction [L], and t is the time [T]. The subscripts 1 and 2 refer to the two different kinetics sites, respectively. The mass transfer between soil solution and both S_1 and S_2 sites (Šimůnek and van Genuchten, 2008) is quantified using Eq. (4):

$$\rho_b \frac{\partial S}{\partial t} = \rho_b \frac{\partial (S_1 + S_2)}{\partial t} = \theta \psi_t k_{att} C - \rho_b k_{det} S_1 + \theta \psi_x k_{str} C \quad (4)$$

where k_{att} and k_{det} are the attachment and detachment rate coefficients, respectively [T^{-1}], ψ_t, and ψ_x are time- or depth-dependent parameters describing bacteria deposition due to retention by the solid phases. Adamczyk et al. (1983) suggested Langmuirian dynamics for ψ_t to explain blocking phenomena and Bradford et al. (2003) proposed a depth-dependent blocking coefficient for straining process (ψ_x), thus a flexible function to account for time- and depth-dependent bacteria deposition behavior (Eqs. 5 and 6, respectively).

$$\psi_t = 1 - \frac{S}{S_{max}} \quad (5)$$

$$\psi_x = \left(\frac{d_c + z}{d_c} \right)^{-\beta} \quad (6)$$

$$\psi_s = \left(1 - \frac{S}{S_{max}} \right) \left(\frac{d_c + z}{d_c} \right)^{-\beta} \quad (7)$$

In these equations, S is the solid phase concentration [N_c M^{-1}], S_{max} is the maximum solid phase concentration [N_c M^{-1}] of colloids on sorption sites, d_c is the mean diameter of sand particles [L], z is the coordination location where the straining process begins, and β was fixed at 0.43, as an empirical factor controlling the shape of the spatial distribution [−], suggested by Bradford et al. (2003).

The Akaike criterion (AIC) (Hurvich, 1989) and the correlation coefficients (R^2) (Willmott, 1982) are reported based on HYDRUS outputs to showcase the fitting performance.

$$AIC = n \ln \left(\frac{RSS}{n} \right) + 2n_p + \frac{2n_p (n_p + 1)}{n - n_p - 1} \quad (8)$$

$$R^2 = 1 - \frac{\sum_{i=1}^{n} (P_i - O_i)^2}{\sum_{i=1}^{n} (O_i - \bar{O}_i)^2} \quad (9)$$

where RSS is the residual sum of squares, n and n_p are number of measurements and model parameters, respectively, O_i, P_i, and $\bar{O}_i$ respectively represent the observed, predicted, and the average of either

Table 1
Physical and chemical properties of soil in this study.

Soil type	Texture	Sand (%)	Clay (%)	Silt (%)	pH	EC (dS m^{-1})	OC (g 100 g^{-1})	CEC ($Cmol_c$ kg^{-1})
Wettable	Silt loam	30.4	4.3	65.3	7.80	0.57	0.32	14.95
Water repellent	Silt loam	10.4	17.5	72.0	7.30	1.218	4.93	36.52

Table 2
Optimized hydraulic properties of the wettable and water-repellent soil related to *E. coli* and *R. erythropolis* columns for simultaneous simulation of dry (Pulse I) and wet infiltration (Pulse II) together. θ_s: saturated water content, K_s: saturated hydraulic conductivity, λ: dispersivity, θ_{im}: immobile water content, α: mass transfer coefficient for Br^- exchanged between mobile and immobile liquid regions. R^2 denotes the correlation between the observed Br^- breakthrough curves and the fitted ones. AIC is the Akaike criterion. The figures in the parentheses represent the standard deviation.

	K_s (cm min^{-1})	θ_s (cm^3 cm^{-3})	θ_{im} (cm^3 cm^{-3})	α (min^{-1})	λ (cm)	R^2	AIC
Wettable soil							
E. coli	0.823 (±0.08)	0.638 (±0.06)	0.01 (±0.07)	28.6 (±7.7)	8.25 (±0.51)	0.92 (±0.01)	−180.66 (±40.81)
R. erythropolis	0.897 (±0.02)	0.688 (±0.03)	0.01 (±0.008)	11.2 (±3.87)	10.2 (±5.01)	0.89 (±0.008)	−233.9 (±3.66)
Water-repellent soil							
E. coli	0.63 (±0.06)	0.78 (±0.04)	0.35 (±0.04)	79.67 (±51.4)	24.68 (±9.75)	0.91 (±0.01)	−273.86 (±58.03)
R. erythropolis	0.77 (±0.09)	0.57 (±0.11)	0.27 (±0.05)	11.66 (±9.96)	5.58 (±3.44)	0.89 (±0.01)	−247.4 (±30.80)

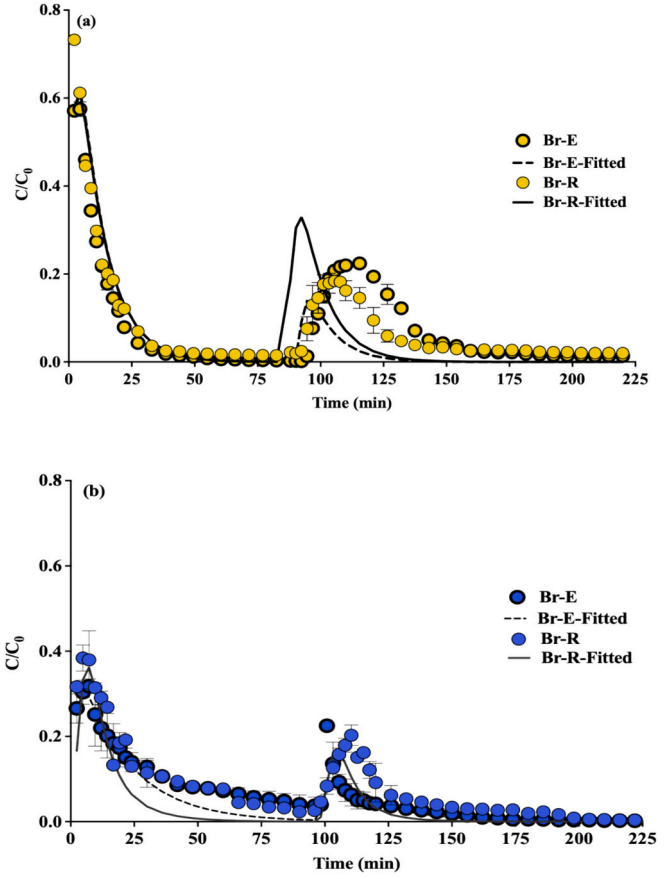

Fig. 1. Bromide (Br) breakthrough curves through (a) wettable (b) and water-repellent soil columns optimized in simultaneous simulation of two pulses (0 to 225) for *Escherichia coli* (E) and *Rhodococcus erythropolis* (R) columns, respectively. Symbols are experimental data from Sepehrnia et al. (2019). The bars represent the standard deviation.

hydraulic properties or bacteria concentration.

3. Results

3.1. Soil hydraulic properties

Further analysis of Sepehrnia et al. (2019) showed that the bimodal pore systems of the soil fit very well with Durner's model (Durner, 1994) implemented in HYDRUS. In Figs. 1 to 4, two simulations of Br^- and bacteria breakthrough curves using HYDRUS are shown: (i) simultaneous simulation of the injected pulses together (Figs. 1 and 3); (ii) separate predictions for either pulses (Figs. 2 and 4). These show the hydraulic properties and Br^- transport were well-captured. The AIC values ranged from −80.79 to −273.86 (Tables 2 and 3). By extension, for the wettable soil, modeling of the breakthrough curves (BTCs) of Br^- in the first pulse fit well to the experimental data, with a slight deviation in the second pulse around the second peak (Figs. 1a-b). In contrast, for the water-repellent soil, the simulation of Br^- transport in each pulse separately was more accurate than simulating both pulses together (Fig. 2).

The optimized hydraulic properties of the soils packed in the columns are also presented in Tables 2 and 3. The AIC and R^2 values indicated satisfactory performance of the model. In the simultaneous optimization of the data, the values of K_s in the wettable soil were slightly higher than the water-repellent counterpart, however, the θ_s, θ_{im}, α, and λ values were significantly higher for the water-repellent soil than the wettable soil (Table 2).

There was agreement in simulations whether they separated or grouped the dry and wet pulses (Tables 2 and 3). By extension, for either pulse in the wettable soil, similar results were found for the values of K_s and θ_s if compared with the first simulation (Table 3). This was also true for the water-repellent soil with a slightly greater variation of K_s values. However, significant differences between the soils or the bacteria were discovered from the values of θ_{im}, α, and λ if the simulation of either pulse were compared. By extension of the separate simulation, the results for the wettable soil showed that the values of *Ks* (e.g., 1.05 cm min^{-1}) and θ_{im} (0.14 cm^3 cm^{-3}) were estimated to be higher in the first pulse compared to the second pulse (0.83 cm min^{-1} and 0.001 cm^3 cm^{-3}). But the θ_s values were simulated to be higher in the second pulse. This trend was totally inversed for the parameters of the water-repellent soil if the pulses were compared (Table 3).

The α and λ values derived from the data of the hydrophilic *E. coli* columns by HYDRUS were significantly smaller than the hydrophobic *R. erythropolis* counterparts in the first pulse of the wettable soil. However, in the second pulse, there were no significant differences observed between them if the wettable soil is still considered (Table 3). Interestingly, an opposite trend, with a better contrast, was obtained for the water-repellent soil so that higher values were obtained for the *R. erythropolis* columns (Table 3). The θ_{im} value was similar for both *E. coli* and *R. erythropolis* columns (e.g., 0.37), however, it was reduced in the second pulse (Table 3).

3.2. Modeling bacteria transport, retention and release

The data for bacteria were similarly modeled in both pulses together and either pulse separately. Modeling of the bacteria BTCs was successful for both soils (AIC: −161 to −233, R^2: 0.70 and 0.79) when the two pulses were simultaneously simulated (Fig. 3a-d), but the simulation of either pulse separately was only possible for the wettable soil (AIC:

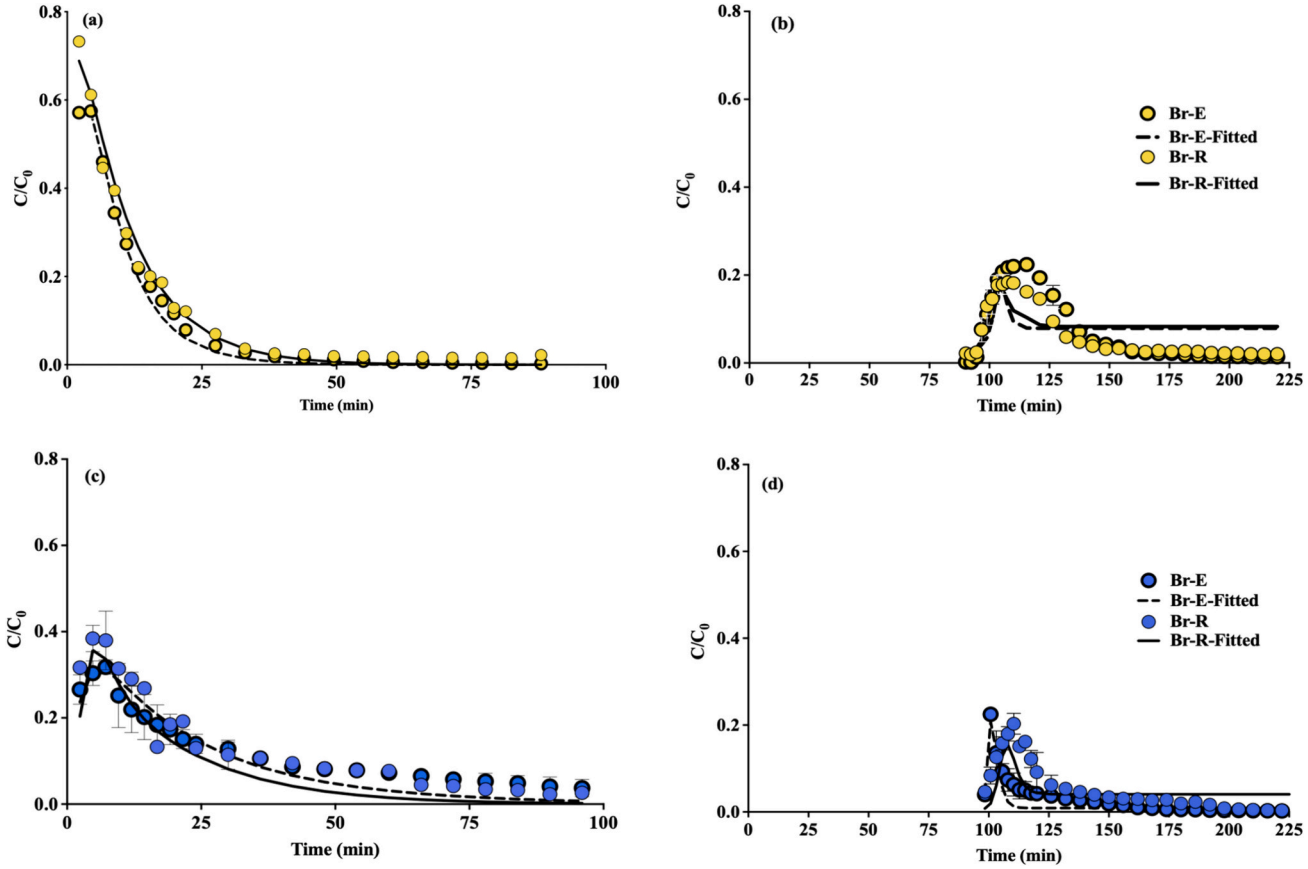

Fig. 2. Bromide (Br) breakthrough curves through (a and b) wettable (c and d) and water-repellent soil columns optimized in separate simulations of pulse I (i.e., 0 to 100 min) and pulse II (i.e., 100 to 225 min) for *Escherichia coli* (E) and *Rhodococcus erythropolis* (R) columns, respectively. Symbols are experimental data from Sepehrnia et al. (2019). The bars represent the standard deviation.

−117 to −181, R^2: 0.48) (Fig. 4 a-d).

The results for the simultaneous modeling of two pulses are presented in Table 4. The values of S_{max}, $k_{att,}$ and k_{str} but not k_{det} and k_{rele} yielded for both bacteria were significantly higher in the wettable soil compared to the water repellent soil (Table 4). The attachment of hydrophobic *R. erythropolis* (82.37 min^{-1}) to the wettable soil was higher than hydrophilic *E. coli* (46.11 min^{-1}). However, the detachment of both bacteria (0.09 and 0.20 min^{-1}) and the physical retention (0.20 and 0.30 min^{-1}) were roughly the same, while the physical release of *E. coli* (0.01 min^{-1}) was greater than that for *R. erythropolis* (0.002 min^{-1}).

Unlike the Br^- data, modeling the transport of bacteria for each pulse individually was only possible for the wettable soil, as presented in Table 5. There were significant differences between the pulses for bacteria transport, retention, and release. In the first pulse, the values of k_{att}, and k_{str}, but not S_{max}, k_{det} and k_{rele}, were significantly higher than the second pulse, values. For instance, the k_{att} values in the first pulse for *E. coli* was 7.51 min^{-1} and *R. erythropolis* was 3.17 min^{-1}, while in the second pulse, the values decreased to 0.42 min^{-1} for *E. coli* and 1.5 min^{-1} for *R. erythropolis* (Table 5). Similarly, the k_{str} coefficient for both bacteria were higher than those in the second pulse. However, the S_{max}, k_{det}, and k_{rele} values depended on bacteria strain, with an opposite trend if the two pulses were compared (Table 5). The values of k_{att} and k_{det} coefficients and the values of S_{max} coefficient obtained from the simulation of either pulse (Table 5) were smaller than their corresponding values in the simultaneous modeling (Table 4). However, the values of k_{str} and k_{rele} coefficients showed the opposite trend, with higher values in the separate modeling compared to simultaneous modeling (Tables 4 and 5).

4. Discussion

4.1. Changes of soil hydraulic properties

Building on the unique experimental results in Sepehrnia et al. (2019), the modeling approaches in the current study clearly showed the effect of the initial dry conditions and the dynamics of wettability of the two soils. The higher K_s and smaller θ_{im} values indicated greater water infiltration and flux into the wettable soil while the opposite trend (i.e., smaller K_s and the higher θ_{im} values) for the water-repellent soil illustrated the effects of water repellency (Dexter, 1988; Nimmo, 2012). Water-repellent soils have smaller K_s compared to wettable soils, whereas, after water repellency cessation, the K_s of such soils has been observed to increase considerably (Bachmann et al., 2007; Hardie et al., 2011; Sepehrnia and Bachmann, 2022). Modeling captured the breakdown of repellency and, the breakdown of water repellency (particularly in the second pulse) could cause the associated higher values of θ_s and K_s in the water-repellent soil (Tables 2 and 3). With this breakdown in the repellency, the water saturation degree could have been increased due to the higher OC content (Table 1). These findings illustrate the effect of the simultaneous presence and absence of water repellency with a wetting front of water advancing through the soil. The data reported in Tables 2 and 3 are comparable with previous studies concerning bacteria and colloids transport (Bai et al., 2023; Bai et al., 2017; Bai et al., 2016; Eisfeld et al., 2022; Spanik et al., 2021; Zhou et al., 2023). Wang et al. (2018) confirmed the performance of HYDRUS-1D in simulating water movements (both horizontal and vertical infiltration) in water-repellent soils using two types of columns. Their study showed that as the intensity of water repellency in soils increased, the values of *Ks*, θ_s, and θ_r decreased. Furthermore, Diamantopoulos et al. (2013) conducted

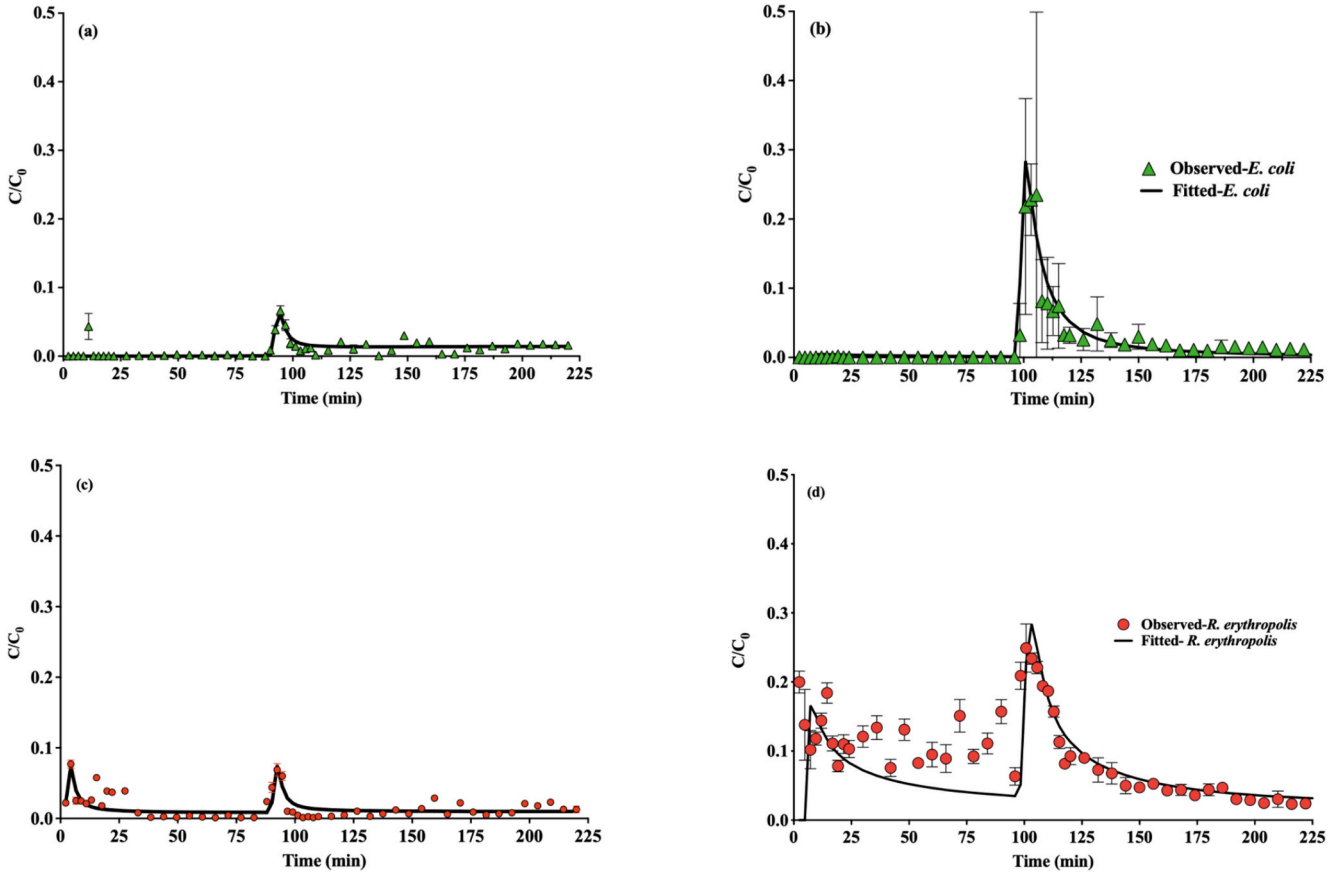

Fig. 3. Bacteria breakthrough curves through (a and c) wettable and (b and d) water-repellent soil columns optimized in simultaneous simulation of two pulses (0 to 225 min) for *Escherichia coli* (*E. coli*) and *Rhodococcus erythropolis* (*R. erythropolis*), respectively. Symbols are experimental data from Sepehrnia et al. (2019). The bars represent the standard deviation.

multistep inflow/outflow experiments with water and ethanol on four substrates, inducing water repellency by adding hydrophobic sand in varying ratios. They performed these experiments under initially dry and saturated conditions to account for hysteresis and used inverse parameter estimation to obtain soil hydraulic properties. Their results demonstrated that soil water repellency affects hydraulic properties on the wetting curve, contributing to hysteresis, and that artificial mixtures with higher fractions of hydrophobic substances exhibited a greater impact of water repellency on hydraulic properties compared to naturally repellent soils. Wang et al. (2021) used HYDRUS-1D to study summer maize growth in water-repellent soils, analysing soil water content and root water uptake across five levels of soil water repellency in a two-year field experiment. While theoretically, the θ_s values should be the same for both control and water-repellent soils with similar texture (sandy loam), minor differences were observed in the measurements. They also reported that the values of *Ks* decreased with increasing water repellency (measured using WDPT).

The higher values of θ_{im} demonstrated preferential water flow and likely formation of more stagnant water-pockets in the water-repellent soil (Nimmo, 2012), while the effects were reduced in the second pulse when the degree of water saturation increased, and water repellency ceased or minimized (Table 3). This pattern was even observed for the wettable soil if the values of θ_{im} in first and the second pulses are compared (Table 3), which likely illustrated the effect of local preferential water flow at short distances occurs in dry conditions (Beven and Germann, 2013; Clothier et al., 2008; Hardie et al., 2011). Furthermore, the higher values of α but smaller θ_{im} values (11.2–79.67 min^{-1}, and 0.01–0.35 $cm^3\ cm^{-3}$, Table 2) compared to Zhou et al.'s (2023) data for three sandy soils profiles (4.61×10^{-6}-7.0×10^{-3} min^{-1}, and 0.08–0.6 $cm^3\ cm^{-3}$), indicates the importance of soil textures on bacteria mass transfer (slit loam vs. sandy). Additionally, the higher values of λ also show that Br^- and bacteria might experience greater tortuosity in these silt loam soils compared to previous studies focused on natural aquifer sand materials (e.g., Eisfeld et al., 2022; Zhou et al., 2023).

Our modeling procedures also showed an excellent correspondence between α and λ, demonstrating that hydrophobic and hydrophilic bacterial strains respond differently to soil and initial hydraulic conditions. The higher values of α and λ for Br^- in the *E. coli* columns compared to *R. erythropolis* in simultaneous modeling for the two soils possibly illustrate the effect of flow turbulence and hydrodynamic variations on bacterial size and shape (Bradford et al., 2007; Lauga, 2016; Wolgemuth, 2008). *Escherichia coli*, being larger, likely exhibited greater susceptibility to hydrodynamic torque changes compared to *R. erythropolis,* particularly in the water-repellent soil (Bai et al., 2017; Torkzaban et al., 2007). This finding is also reiterated in the separate pulse modeling for the water-repellent soil that could also show greater hydraulic instability compared to wettable soils (Nimmo, 2012) given that a water-repellent soil (CA > 0°) exhibits lower soil water tension compared to the same soil with hydrophilic properties (CA = 0°), for a particular pore size distribution and water content (Gaj et al., 2019). Similarly, considering the size of bacteria, Spanik et al. (2021) reported higher λ values (1.93 vs. 1.56 cm) for large microspheres (1 μm) with amine-modified latex and anionic carboxylate-modified latex than smaller ones (0.2 μm) under both favorable and unfavorable attachment conditions in leaching a discrete sandstone. When soil type is considered, particularly sand content, we obtained greater values for λ (5.58–24.68 cm) compared to Spanik et al. (2021) (λ: 1.51–1.93 cm). Similarly, for the values of α (11.2–79.67 min^{-1}, Table 2), our results are

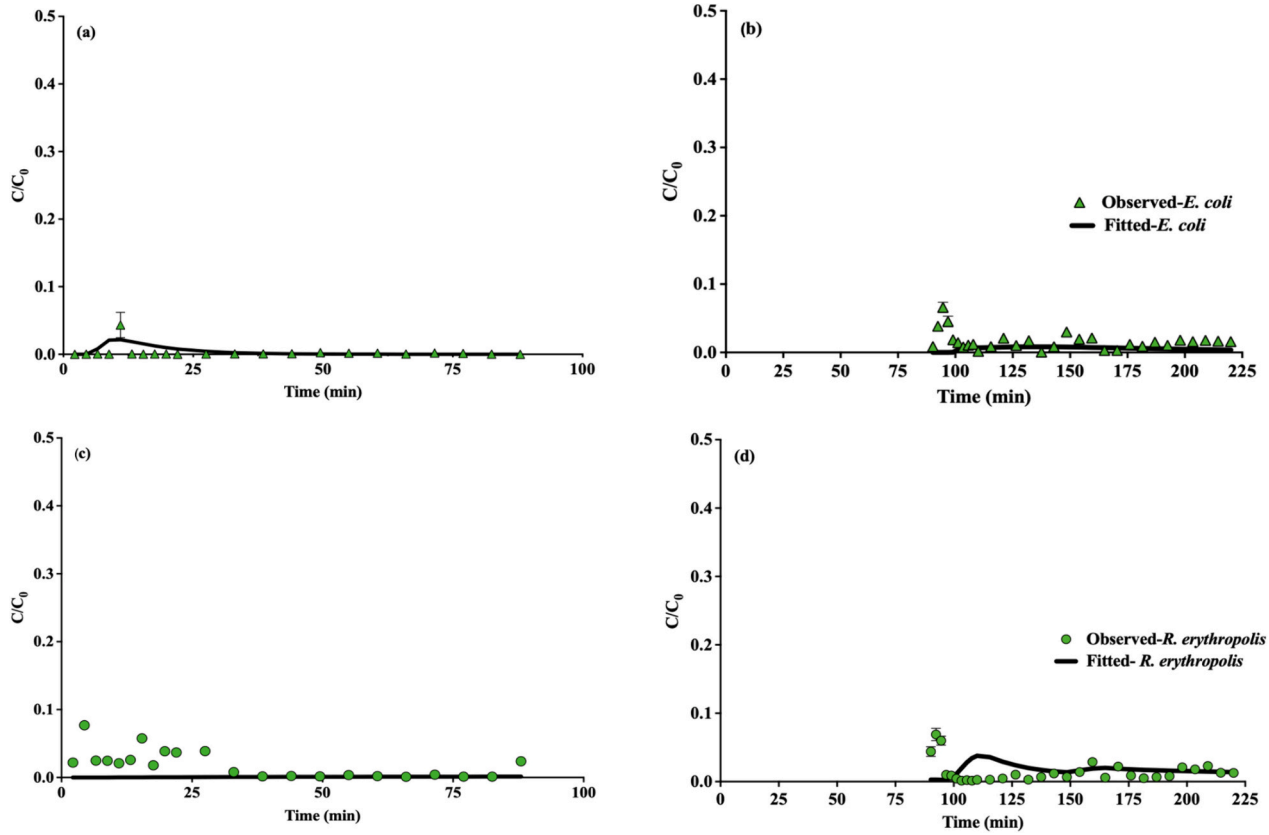

Fig. 4. Bacteria breakthrough curves through wettable soil columns optimized in separate simulations of pulse I (i.e., 0 to ~90 min) and pulse II (c and d, i.e., ~90 to 225 min) for (a and b) *E. coli* and (c and d) *R. erythropolis*. The latter simulation was not achieved for water-repellent soil. Symbols are experimental data from Sepehrnia et al. (2019). The bars represent the standard deviation.

Table 3
Optimized hydraulic properties of the wettable and water-repellent soil columns for separate simulation of dry (Pulse I) and wet infiltration (Pulse II). θ_s: saturated water content, K_s: saturated hydraulic conductivity, λ: dispersivity, θ_{im}: immobile water content, α: mass transfer coefficient for Br^- exchanged between mobile and immobile liquid regions. R^2 donates the correlation between the observed Br^- breakthrough curves and the fitted ones. AIC is the Akaike criterion. The figures in the parentheses represent the standard deviation.

	K_s (cm min^{-1})	θ_s (cm^3 cm^{-3})	θ_{im} (cm^3 cm^{-3})	α (min^{-1})	λ (cm)	R^2	AIC
Wettable soil							
	Pulse 1						
E. coli	0.99	0.63	0.10	1.00	5.42	0.99	−165.1
	(±0.04)	(±0.03)	(±0.04)	(±0.65)	(±1.23)		
R. erythropolis	1.05	0.69	0.14	16.69	16.51	0.99	−124.0
	(±0.12)	(±0.01)	(±0.11)	(±2.86)	(±9.27)		
	Pulse 2						
E. coli	0.79	0.72	0.011	2.56	0.19	0.61	−123.0
	(±0.01)	(±0.02)	(±0.01)	(±4.05)	(±0.12)		
R. erythropolis	0.83	0.74	0.001	2.98	0.55	0.70	−112.4
	(±0.07)	(±0.04)	(±0.001)	(±5.01)	(±0.14)		
Water repellent soil							
	Pulse 1						
E. coli	0.52	0.69	0.37	260.06	23.3	0.97	−98.41
	(±0.26)	(±0.32)	(±0.23)	(±43.2)	(±12.82)		
R. erythropolis	0.64	0.73	0.34	11.81	7.80	0.91	−80.79
	(±0.16)	(±0.15)	(±0.08)	(±20.38)	(±6.79)		
	Pulse 2						
E. coli	1.68	0.54	0.102	61.31	1.68	0.91	−106.3
	(±0.14)	(±0.008)	(±0.11)	(±27.5)	(±0.44)		
R. erythropolis	0.81	0.56	0.003	0.06	0.701	0.67	−125.6
	(±0.06)	(±0.03)	(±0.006)	(±0.06)	(±0.47)		

Table 4
Transport and retention parameters (maximum solid phase concentration of deposited bacteria S_{max}, attachment coefficient k_{att}, detachment coefficient k_{det}, straining coefficient k_{str}, and physical release coefficient k_{rele}) fitted using the effluent and the deposition concentrations of bacteria for the wettable and water repellent soil. And AIC is the Akaike criterion. The figures in the parentheses are the standard deviation.

Soil	Bacteria/parameter	S_{max2} (−)	k_{att}	k_{det}	k_{str}	k_{rele}	R^2	AIC
			(min^{-1})					
Wettable	*E. coli*	0.315 (±0.19)	46.11 (±13.00)	0.09 (±0.11)	0.20 (±0.052)	0.01 (±0.001)	0.71 (±0.046)	−233.13 (±28.56)
	R. erythropolis	0.300 (±0.012)	82.40 (±38.95)	0.20 (±0.116)	0.30 (±0.074)	0.002 (±0.002)	0.70 (±0.033)	−205.26 (±6.99)
Water repellent	*E. coli*	0.26 (±0.22)	4.61 (±2.57)	6.609 (±7.6)	0.0037 (±0.001)	0.166 (±0.14)	0.79 (±0.11)	−233.53 (±78.74)
	R. erythropolis	0.021 (±0.012)	8.318 (±0.888)	52.924 (±41.78)	0.032 (±0.032)	0.046 (±0.031)	0.54 (±0.015)	−161.67 (±5.29)

Table 5
Transport and retention parameters for dry (Pulse I) and wet infiltration (Pulse II) (maximum solid phase concentration of deposited bacteria S_{max}, attachment coefficient k_{att}, detachment coefficient k_{det}, straining coefficient k_{str}, and physical release coefficient k_{rele}) fitted using the effluent and the deposition concentrations of bacteria for the wettable and water repellent soil. AIC is the Akaike criterion. The figures in the parentheses are the standard deviation.

Wettable Soil	Bacteria/parameter	S_{max2} (−)	k_{att}	k_{det}	k_{str}	k_{rele}	R^2	AIC
			(min^{-1})					
Pulse I	*E. coli*	0.01 (±0.01)	7.51 (±6.31)	0.01 (±0.01)	1.31 (±0.40)	2.91 (±1.19)	0.47 (±0.08)	−169.43 (±20.23)
	R. erythropolis	0.002 (±0.001)	3.17 (±1.89)	0.013 (±0.01)	1.85 (±0. 73)	0.74 (±0.23)	0.48 (±0.06)	−17.66 (±5.45)
Pulse II	*E. coli*	0.15 (±0.05)	0.24 (±0.01)	0.044 (±008)	0.001 (±0.002)	0.74 (±0.28)	0.47 (±0.06)	−125.31 (±72.89)
	R. erythropolis	0.013 (±0.012)	1.51 (±1.05)	0.002 (±0.002)	0.74 (±0.17)	1.34 (±0.14)	0.49 (±0.13)	−181.6 (±18.10)

higher compared to Zhou et al. (2023) (α: 4.61 × 10^{-6}-7.0 × 10^{-3} min^{-1}), but we optimized smaller θ_{im} values (0.01–0.35 cm^3 cm^{-3}, Table 2) compared to Zhou et al. (2023) (θ_{im}: 0.08–0.6 cm^3 cm^{-3}).

In the separate modeling for the wettable soil, however, two distinct outcomes were observed for α and λ, demonstrating the influence of bacterial type and soil type. In the initial dry condition (pulse I), the higher wettability and thus significant capillary forces likely resulted in the retention of the larger *E. coli* and restricted its dispersivity and mass transfer. Conversely, *R. erythropolis*, with smaller size, was significantly dispersed throughout the soil even by the thinner water films and facilitating greater mass exchanges (1.00 ± 0.65 vs. 16.69 ± 2.86 min^{-1}, Table 3). In the second pulse, with increases in the thickness of water films and degree of saturation beyond the size of both bacteria, the effect became less significant, and due to the greater stability of water movement in the wettable soil, no substantial difference in bacterial mass transfer coefficients (2.56 ± 4.05 vs. 2.98 ± 5.01 min^{-1}) was observed, while it was still comparable with the first pulse. (e.g., *E. coli*: pulse I: 1.00 ± 0.65 min^{-1} and pulse II: 2.56 ± 4.05 min^{-1}, Table 3).

Additionally, the smaller values of α coefficient for Br^- in both soils illustrate that *R. erythropolis,* possibly due to its size, could have experienced greater preferential transport than *E. coli*. Similarly, studies conducted on wettable and water-repellent sand materials by Sepehrnia et al. (2023) showed that the values of the α coefficient for Br^- in the first pulse were higher due to the initial dry conditions and the tendency for solute exchange with dry pathways in the water-repellent sand. They reported larger values of dispersivity and mass exchange coefficients for the wettable and water-repellent sands, respectively (Sepehrnia et al., 2023).

Overall, while simultaneous modeling of the two pulses could better characterize the effects of soil wettability property, bacteria sizing and hydrophobicity/hydrophilicity, separate modeling of the either pulse clarified the importance of initial water boundary conditions on hydraulic behavior of soils and bacteria fate. These findings are crucial for understanding water movement and contaminant transport in soil ecosystems.

4.2. Consequences of soil water repellency and contrasting hydraulic conditions on bacteria fate

Our modeling also provided new insight into attachment and straining mechanisms depending on the hydrophobicity of either soil or bacteria, building considerably on past research. The small values of S_{max} for the water-repellent versus the similar values of S_{max} for the wettable soil demonstrated the effect of water repellency phenomenon by which fewer retention sites were provided for bacteria although it had a higher clay content than the wettable soil organic matter in soils favors bacterial attachment (Chen et al., 2021; Xu et al., 2019), however, fewer retention sites in the water-repellent soil with higher OC content demonstrated that the quality of organic matter is important in bacteria retention. For instance, Chen et al. (2021) attributed a decrease breakthrough percentage of *E. coli* 652 T7 (for intact and repacked samples) to increases in organic matter quantities (from 2.5 % to 3.8 %), illustrating that organic matter content might be an effective measure for reducing bacterial movement in soils. Similarly, Xu et al. (2019) examined how mineral-associated organic matter (MOM) and dissolved organic matter (DOM) affect hydroxyapatite nanoparticle (nHAP) transport through loamy soil under saturated flow. They found that nHAP mobility in natural loamy soil was limited primarily due to mechanical straining from nanoparticle aggregation and surface deposition enhanced by MOM, while DOM facilitated nHAP transport due to electrostatic/electrosteric repulsion. Interestingly, the higher S_{max} for *E. coli* than *R. erythropolis* in the water-repellent soil could indicate the effect of hydrophobicity interactions between bacteria and soil. Flagella phases and the methylation of the flagella can significantly affect bacteria movement and deposition in porous media (Zheng et al., 2022). Given that, hydrophobicity of the outer surface of the flagella might be a potential reason for the increased *E. coli* transport (Zhang et al., 2021).

The higher values of k_{att} (e.g., 46.11 and 82.4 min^{-1} or 4.61 and 8.32 min^{-1}) compared to k_{str} values (0.19 and 0.3 min^{-1} or 0.004 and 0.032 min^{-1}) demonstrated that attachment was the dominant bacteria retention mechanism for both strains. Additionally, the higher values of

k_{det} compared to k_{rele} values of bacteria indicated the importance of physicochemical attachment relative to physical straining (Bradford et al., 2015; Bradford et al., 2013; Torkzaban et al., 2007). Researchers have reported the k_{att} values from 4.54×10^{-5} to 1.80×10^{-1} min^{-1}, and for k_{det} from 1.00×10^{-6} to 9.14×10^{-1} min^{-1} in leaching experiments of sandy soil columns (Bai et al., 2016; Gargiulo et al., 2008; Sepehrnia et al., 2017). In a lysimeter study on the impact of biochar and wastewater on wettable soil under subsurface drip irrigation, HYDRUS-2D determined that the attachment, straining, and detachment coefficients for faecal coliform bacteria ranged from 5.3×10^{-9} to 3.08×10^{-5}, 0.012 to 0.038, and 0.003 to 0.01 min^{-1}, respectively (Teshnizi et al., 2023). Chen et al. (2021) concluded that *E. coli 652 T7* transport increased through soil depths with silty clay loam texture in intact and disturbed samples. For disturbed soils samples, the values of k_{att} ranged from 2.25 to 36.08 min^{-1} and k_{det} from 1.50×10^{-3} to 1.7×10^{-4} min^{-1} from the surface to 20 cm depth. For intact soil samples, they reported the values of k_{att} between 2.00 and 24.8 min^{-1}, with the values from 6.70×10^{-4} to 1.8×10^{-2} min^{-1}. Spanik et al. (2021) evaluated the possibility of reversible and irreversible attachment of the microspheres (0.2 μm and 1 μm in size) through a sandstone using the two-site attachment model (i.e., reversible and irreversible sites). For favorable attachment scenario, Spanik et al. (2021) found irreversible attachment (i.e., k_{att}) were higher and reversible retention (i.e., k_{str}) was lower than for unfavorable attachment. This result is consistent with our data for high bacteria attachment yielded for both soils, particularly the wettable soil in pulse I (i.e., with in initial dry condition and high hydrophilicity), while thanks to water repellency and the wet-stated of pulse II, bacteria attachment was less favorable and that was reflected with the high detachment coefficient values.

Our previous systematic research with a similar experimental set-up illustrated that in dry wettable sand medium, *E. coli* fate was predominantly governed by attachment, while *R. erythropolis* primarily relied on straining (Sepehrnia et al., 2023). Upon wetting, the prevailing mechanisms between these bacteria underwent a switch; in the water-repellent sand, both bacteria attachments significantly decreased, thus highlighting straining as the primary mechanism for retention (Sepehrnia et al., 2023). Gao et al. (2021) explored *E. coli* transport through microplastics-affected sand columns and found that the k_{str} coefficients in reversible physical retention (e.g., 0.47–2.64 min^{-1}) were generally much greater than the k_{att} in irreversible physicochemical attachment (0.08–1.1 min^{-1}) with the optimized S_{max} values ranging from 0.07 and 1.4 mg g^{-1} in pure quartz sand columns.

Surprisingly, the changes of k_{det} and k_{rele} clearly differentiated the processes occurring for bacteria that depended on soil wettability, bacteria sizing, and hydrophobicity/hydrophilicity. *Rhodococcus erythropolis* detached more but *E. coli* released, and the rates were enhanced due to water repellency (Table 4). This result proves that variations in the air-water interface (AWI) and the solid-water interface (SWI) in both pulses I and II coupled with the changes of water repellency and dryness systemically impact bacteria detachment and release mechanisms, reflecting changes in bacteria partitioning between the SWI, AWI, soil solution phase and locations where bacteria physically retained (e.g., grain-grain contacts). By extension, if the strains are considered, *R. erythropolis*, with a smaller size, had a greater chance to attach to the soil particle surfaces or be entrapped due to capillary forces in pulse I (Sepehrnia et al., 2023; Sepehrnia et al., 2018a). However, due to the reduced capillary forces and weak surface adsorption energies of the water repellent soil (Bachmann and McHale, 2009; Bai et al., 2017; Bai et al., 2016; Sepehrnia et al., 2023; Sepehrnia et al., 2019), hydrophobic *R. erythropolis* was highly detached. The greater release rates of hydrophilic *E. coli* indicated they experienced more capillary forces, likely due to their more hydrophilic surface than *R. erythropolis*, but they also experienced greater hydrodynamic stresses due to larger size after the breakdown of water repellency by which bacteria were more pushed to the soil solution. Therefore, the k_{det} and k_{rele} coefficients demonstrated the effects of size and hydrophobicity/hydrophilicity on bacteria fate in the water repellent soil. These effects were also apparent for the wettable soil (e.g., k_{rele}: 0.01 *E. coli* vs. 0.002 min^{-1} *R. erythropolis*), although strong adsorption forces of the wettable soil probably caused less physicochemical detachment and also minimized the physical release of bacteria. The data were also illustrated through the separate modeling of either pulse for the wettable soil, with a better contrast for the dry condition although further research is necessary to enhance the flexibility of HYDRUS for modeling bacteria under such extreme conditions of the water-repellent soils. Similarly, Bradford et al. (2015) numerically optimized *Escherichia coli D21g* release from the SWI and the AWI using sand columns (120 μm), and they found that imbibition to a higher water content resulted in greater colloid release due to increased flow rates and more destruction of the AWI. While Bradford et al. (2015)'s data addresses k_{det} from sand materials, it coincides with our modeling approach for the natural soils with silt loam texture. Additionally, we could robustly differentiate the impacts of the k_{det} and k_{rele} coefficients for the bacteria and soils.

With these, it can be ascertained that the mechanisms of bacteria retention may vary between natural soils and clean bed systems in the lab even under similar boundary conditions. Notwithstanding, we believe the contrast in the textures can be the main important factor (e.g., silt loam vs. clean sand media) as it contributes to micro-scale hydrodynamic instability and thus complex movements of water, solute, and bacteria when it is coupled with water repellency (Gaj et al., 2019; Wang et al., 2018). These results therefore indicate that soil surface wettability, mainly governed by SWI, plays a crucial role in controlling the transport and partitioning of bacteria into soil solution. This effect becomes especially pronounced with significant variations in AWI, ranging from very dry to highly saturated conditions. Additionally, the characteristics of bacteria themselves are key in influencing their detachment and/or release.

4.3. Bacteria mortality effects

Considering the experimental duration (225 min), the possibility of bacteria mortality and growth in water and soil systems existed, which could have affected the performance of the HYDRUS 1-D model. We assessed the factors by taking mortality into account in the liquid and solid phases (μ_w and μ_s, respectively), however, the μ value was equal to 10^{-4} min^{-1}. The inclusion of the mortality coefficient in either the solid or liquid phase for estimation purposes rendered the model inexecutable (an increased number of parameters for estimation). Nevertheless, the R^2 values proved unpromising, merely amounting to 0.01. Therefore, everything in the case of bacterial mortality and growth that occurred in the studied systems over the duration of the experiment was assumed to have a constant effect. Primarily, the experimental data from Sepehrnia et al. (2019) (e.g., *E. coli*; 36 % in the wettable soil and 96 % in the water repellent soil vs. *R. erythropolis*: 78 % and 86 %, respectively) showed that soil wettability, initial boundary conditions, water flow characteristics, and bacteria strains can highly affect the mass recovery rate of bacteria and that might consequently affect bacteria survival. The values of k_{att} coefficients in the modeling provided a robust indication that bacteria had been highly attached to the surfaces and interfaces (particularly during the initial stages of the wettable soil), and the attachment effects were likely much greater than bacterial mortality. Similarly, Barrios et al. (2021) investigated how manure application affects the subsurface transport of four antibiotic resistance genes in a sandy loam soil and reported that the k_{att} coefficients for the treated soils were five to six orders of magnitude higher than in the control soil, while detachment and decay coefficients remained largely unchanged for control and treatment columns (k_{det}: 1.63×10^{-7} to 1.94×10^{-6}, and μs: 3.50×10^{-7} to 2.04×10^{-6} min^{-1}). However, studies have demonstrated that clays enhance bacterial survival and metabolic activity more than silts and sands, primarily through attachment, rather than nutrient supply from natural organic matter. And, removing Fe/Al (hydro) oxides from soil particles improves bacterial survival, highlighting the

importance of soil chemical composition in pathogen persistence (Liu et al., 2017). Teshnizi et al. (2023) using modeling approach by HYDRUS-2D concluded that the high flow rate of water forced bacteria into the biochar pore spaces and resulted in a decrease of bacteria die-off. Further Fexperimental studies have also shown that bacteria can survive for long-time in soil and it is an important factor for bacteria fate (e.g., Bradford et al., 2013; Çekiç et al., 2017; Liu et al., 2017; Unc and Goss, 2003). Çekiç et al. (2017) determined the persistence of manure-borne generic *E. coli* under laboratory and field conditions and reported that in field trials, the longest persistence occurred during summer and fall, lasting up to 112 and 280 days, respectively. They reported a decay rate ranging from 0.02 to 0.04 (log CFU [colony forming unit] per day). In microcosms, *E. coli* lasted until day 210 at 30 °C and day 420 at 20 °C.

Finally, we believe that the high coefficients for bacteria attachment thus suggest that bacterial mortality is of less importance, and attachment was the dominant mechanism for bacteria retention in the soils. Notwithstanding, further studies are needed to evaluate this at the soil particle or smaller scales, e.g., to differentiate the discrepancies between highly alive/dead attached bacteria and modeling results.

5. Conclusions

Apart from the extreme conditions of a dry pulse of water through water repellent soil, the HYDRUS model captured the fate and transport of different bacteria in soil well. Our data confirmed that physicochemical attachment was the predominant mechanism for bacteria retention in either wettable or water repellent soils. Attachment even remained for the wettable soil in modeling the pulses separately. However, this was not the case for the water-repellent soil, making it challenging to determine due to the high rate of mass transfer in the dry pulse or after water repellency cessation ascertained from Br^- data. Further research is thus necessary to enhance the flexibility of HYDRUS for such extreme conditions. Surprisingly, the physicochemical detachment and physical release clarified the effects of soil wettability, size, and hydrophobicity/hydrophilicity of bacteria.

Overall, the results supported our recent systematic study on sandy media and highlighted the significant roles of natural soil conditions and properties including initial water content as well as wettability in controlling or accelerating bacteria transport. Research focused on the effects of bacteria surface properties at the nanoscale could improve understanding of bacterial macromolecule roles on their transport and survival in very dry conditions.

CRediT authorship contribution statement

Nasrollah Sepehrnia: Writing – review & editing, Writing – original draft, Software, Resources, Project administration, Methodology, Investigation, Funding acquisition, Formal analysis, Data curation, Conceptualization. **Forough Abbasi Teshnizi:** Software, Methodology, Investigation, Formal analysis, Data curation. **Paul Hallett:** Writing – review & editing, Visualization, Validation, Supervision. **Mark Coyne:** Writing – review & editing, Visualization, Validation, Supervision. **Nima Shokri:** Writing – review & editing, Visualization, Validation, Supervision. **Stephan Peth:** Writing – review & editing, Visualization, Validation, Supervision.

Declaration of competing interest

The authors declare that they have no known competing financial interests or personal relationships that could have appeared to influence the work reported in this paper.

Data availability

Data will be made available on request.

Acknowledgements

This project has received funding from the European Union's Horizon 2020 research and innovation programme under the Marie Skłodowska-Curie Grant agreement no. 101026287. We acknowledge University of Aberdeen, UK and Isfahan University of Technology, Iran for supporting this project.

References

Adamczyk, Z., Dabros, T., Czarnecki, J., Van De Ven, T.G., 1983. Particle transfer to solid surfaces. Adv. Colloid Interf. Sci. 19, 183–252.
Alegbeleye, O., Sant'Ana, A.S., 2023. Survival behavior of six enterotoxigenic Escherichia coli strains in soil and biochar-amended soils. Environ. Res. 223, 115443.
Bachmann, J., McHale, G., 2009. Superhydrophobic surfaces: a model approach to predict contact angle and surface energy of soil particles. Eur. J. Soil Sci. 60, 420–430.
Bachmann, J., Deurer, M., Arye, G., 2007. Modeling water movement in heterogeneous water-repellent soil: 1. Development of a contact angle–dependent water-retention model. Vadose Zone J. 6, 436–445.
Bachmann, J., Söffker, S., Sepehrnia, N., Goebel, M.O., Woche, S.K., 2021. The effect of temperature and wetting–drying cycles on soil wettability: dynamic molecular restructuring processes at the solid–water–air interface. Eur. J. Soil Sci. 72, 2180–2198.
Bai, H., Cochet, N., Pauss, A., Lamy, E., 2016. Bacteria cell properties and grain size impact on bacteria transport and deposition in porous media. Colloids Surf. B: Biointerfaces 139, 148–155.
Bai, H., Cochet, N., Pauss, A., Lamy, E., 2017. DLVO, hydrophobic, capillary and hydrodynamic forces acting on bacteria at solid-air-water interfaces: their relative impact on bacteria deposition mechanisms in unsaturated porous media. Colloids Surf. B: Biointerfaces 150, 41–49.
Bai, H., Zhang, Q., Zhou, X., Chen, J., Chen, Z., Liu, Z., Yan, J., Wang, J., 2023. Removal of fluoroquinolone antibiotics by adsorption of dopamine-modified biochar aerogel. Korean J. Chem. Eng. 40, 215–222.
Barrios, R.E., Bartelt-Hunt, S.L., Li, Y., Li, X., 2021. Modeling the vertical transport of antibiotic resistance genes in agricultural soils following manure application. Environ. Pollut. 285, 117480.
Beven, K., Germann, P., 2013. Macropores and water flow in soils revisited. Water Resour. Res. 49, 3071–3092.
Bradford, S.A., Simunek, J., Bettahar, M., Van Genuchten, M.T., Yates, S.R., 2003. Modeling colloid attachment, straining, and exclusion in saturated porous media. Environ. Sci. Technol. 37, 2242–2250.
Bradford, S.A., Torkzaban, S., Walker, S.L., 2007. Coupling of Physical and Chemical Mechanisms of Colloid Straining in Saturated Porous Media, 41, pp. 3012–3024. https://doi.org/10.1016/j.watres.2007.03.030.
Bradford, S.A., Morales, V.L., Zhang, W., Harvey, R.W., Packman, A.I., Mohanram, A., Welty, C., 2013. Transport and fate of microbial pathogens in agricultural settings. Crit. Rev. Environ. Sci. Technol. 43, 775–893.
Bradford, S.A., Wang, Y., Torkzaban, S., Šimůnek, J., 2015. Modeling the release of E. coli D21g with transients in water content. Water Resour. Res. 51, 3303–3316. https://doi.org/10.1002/2014WR016566.
Braun, B., Böckelmann, U., Grohmann, E., Szewzyk, U., 2010. Bacterial soil communities affected by water-repellency. Geoderma 158, 343–351. https://doi.org/10.1016/j.geoderma.2010.06.001.
Çekiç, S.K., De, J., Jubair, M., Schneider, K.R., 2017. Persistence of indigenous Escherichia coli in raw bovine manure-amended soil. J. Food Prot. 80, 1562–1573.
Chen, J., Yang, L., Chen, X., Ripp, S., Radosevich, M., Zhuang, J., 2021. Bacterial mobility facilitated by soil depth and intact structure. Soil Tillage Res. 209, 104911.
Clothier, B.E., Green, S.R., Deurer, M., 2008. Preferential flow and transport in soil: progress and prognosis. Eur. J. Soil Sci. 59, 2–13.
Dexter, A.R., 1988. Advances in characterization of soil structure. Soil Tillage Res. 11, 199–238.
Diamantopoulos, E., Durner, W., Reszkowska, A., Bachmann, J., 2013. Effect of soil water repellency on soil hydraulic properties estimated under dynamic conditions. J. Hydrol. 486, 175–186.
Durner, W., 1994. Hydraulic conductivity estimation for soils with heterogeneous pore structure. Water Resour. Res. 30, 211–223.
Eisfeld, C., Schijven, J.F., van der Wolf, J.M., Medema, G., Kruisdijk, E., van Breukelen, B.M., 2022. Removal of bacterial plant pathogens in columns filled with quartz and natural sediments under anoxic and oxygenated conditions. Water Res. 220, 118724.
Fomina, M., Skorochod, I., 2020. Microbial interaction with clay minerals and its environmental and biotechnological implications. Minerals 10, 861.
Gaj, M., Lamparter, A., Woche, S.K., Bachmann, J., McDonnell, J.J., Stange, C.F., 2019. The role of matric potential, solid interfacial chemistry, and wettability on isotopic equilibrium fractionation. Vadose Zone J. 18, 1–11.
Gao, M., Peng, H., Xiao, L., 2021. The influence of microplastics for the transportation of E. Coli using column model. Sci. Total Environ. 786, 147487.
Gargiulo, G., Bradford, S.A., Simunek, J., Ustohal, P., Vereecken, H., Klumpp, E., 2008. Bacteria transport and deposition under unsaturated flow conditions: the role of water content and bacteria surface hydrophobicity. Vadose Zone J. 7, 406–419.

Ghosh, B., 2023. What Affects the Survival of *E. coli* in Midwest Agricultural Soils? Iowa State University.

Goebel, M.O., Bachmann, J., Reichstein, M., Janssens, I.A., Guggenberger, G., 2011. Soil water repellency and its implications for organic matter decomposition – is there a link to extreme climatic events? Glob. Chang. Biol. 17, 2640–2656. https://doi.org/10.1111/j.1365-2486.2011.02414.x.

Goebel, M.O., Woche, S.K., Abraham, P.M., Schaumann, G.E., Bachmann, J., 2013. Water repellency enhances the deposition of negatively charged hydrophilic colloids in a water-saturated sand matrix. Colloids Surf. A Physicochem. Eng. Asp. 431, 150–160.

Guber, A.K., Karns, J.S., Pachepsky, Y.A., Sadeghi, A.M., Van Kessel, J.S., Dao, T.H., 2007. Comparison of release and transport of manure-borne Escherichia coli and enterococci under grass buffer conditions. Lett. Appl. Microbiol. 44, 161–167. https://doi.org/10.1111/j.1472-765X.2006.02065.x.

Hardie, M.A., Cotching, W.E., Doyle, R.B., Holz, G., Lisson, S., Mattern, K., 2011. Effect of antecedent soil moisture on preferential flow in a texture-contrast soil. J. Hydrol. 398, 191–201.

Hellberg, R.S., Chu, E., 2016. Effects of climate change on the persistence and dispersal of foodborne bacterial pathogens in the outdoor environment: a review. Crit. Rev. Microbiol. 42, 548–572.

Hewelke, E., Gozdowski, D., Korc, M., Małuszyńska, I., BeataGórska, E., Sas, W., Mielnik, L., 2022. Influence of soil moisture on hydrophobicity and water sorptivity of sandy soil no longer under agricultural use. Catena 208, 105780. https://doi.org/10.1016/j.catena.2021.105780.

Hurvich, C.M., Tsai, C.L., 1989. Regression and time series model selection in small samples. Biometrika 76, 297–307. https://doi.org/10.1093/biomet/76.2.297.

IUSS Working Group WRB, 2022. World Reference Base for Soil Resources. International Soil Classification System for Naming Soils and Creating Legends for Soil Maps, International Union of Soil Sciences (IUSS) Vienna, Austria, 2022, 4th edition.

Kang, J.-K., Lee, C.-G., Park, J.-A., Kim, S.-B., Choi, N.-C., Park, S.-J., 2013. Adhesion of bacteria to pyrophyllite clay in aqueous solution. Environ. Technol. 34, 703–710. https://doi.org/10.1080/09593330.2012.715677.

Lauga, E., 2016. Bacterial hydrodynamics. Annu. Rev. Fluid Mech. 48, 105–130.

Limoges, M.A., Neher, D.A., Weicht, T.R., Millner, P.D., Sharma, M., Donnelly, C., 2022. Differential survival of Escherichia coli and Listeria spp. in northeastern US soils amended with dairy manure compost, poultry litter compost, and heat-treated poultry pellets and fate in raw edible radish crops. J. Food Prot. 85, 1708–1715.

Liu, X., Gao, C., Ji, D., Walker, S.L., Huang, Q., Cai, P., 2017. Survival of Escherichia coli O157: H7 in various soil particles: importance of the attached bacterial phenotype. Biol. Fertil. Soils 53, 209–219.

Nakhle, P., Boithias, L., Pando-Bahuon, A., Thammahacksa, C., Gallion, N., Sounyafong, P., Silvera, N., Latsachack, K., Soulileuth, B., Rochelle-Newall, E.J., Marcangeli, Y., 2021. Decay rate of Escherichia coli in a mountainous tropical headwater wetland. Water 13, 2068.

Nimmo, J.R., 2012. Preferential flow occurs in unsaturated conditions. Hydrol. Process. 26, 786–789.

Rodrigues, C.J., de Carvalho, C.C., 2019. Phenotypic adaptations help Rhodococcus erythropolis cells during the degradation of paraffin wax. Biotechnol. J. 14, 1800598.

Sepehrnia, N., Bachmann, J., 2022. Capturing water repellency cessation time by means of characteristic time method. Geoderma 427, 116126.

Sepehrnia, N., Mahboubi, A.A., Mosaddeghi, M.R., Sinejani, A.S., Khodakaramian, G., 2014. Escherichia coli transport through intact gypsiferous and calcareous soils during saturated and unsaturated flows. Geoderma 217, 83–89.

Sepehrnia, N., Memarianfard, L., Moosavi, A.A., Bachmann, J., Guggenberger, G., Rezanezhad, F., 2017. Bacterial mobilization and transport through manure enriched soils: experiment and modeling. J. Environ. Manag. 201, 388–396. https://doi.org/10.1016/j.jenvman.2017.07.009.

Sepehrnia, N., Bachmann, J., Hajabbasi, M.A., Afyuni, M., Horn, M., 2018a. Modeling transport of Escherichia coli and Rhodococcus erythropolis through wettable and repellent porous media. Colloids Surf. B: Biointerfaces 172, 280–287.

Sepehrnia, N., Fishkis, O., Huwe, B., Bachmann, J., 2018b. Natural colloid mobilization and leaching in wettable and water repellent soil under saturated condition. Journal of Hydrology and Hydromechanics 66, 271–278. https://doi.org/10.1515/johh-2017-0058.

Sepehrnia, N., Bachmann, J., Hajabbasi, M.A., Rezanezhad, F., Lichner, L., Hallett, P.D., Coyne, M., 2019. Transport, retention, and release of Escherichia coli and Rhodococcus erythropolis through dry natural soils as affected by water repellency. Sci. Total Environ. 694, 133666.

Sepehrnia, N., Gorakifard, M., Hallett, P.D., Hajabbasi, M.A., Shokri, N., Coyne, M., 2023. Contrasting transport and fate of hydrophilic and hydrophobic bacteria in wettable and water-repellent porous media: straining or attachment? Colloids Surf. B: Biointerfaces 228, 113433.

Šimůnek, J., van Genuchten, M.T., 2008. Modeling nonequilibrium flow and transport processes using HYDRUS. Vadose Zone J. 7, 782–797. https://doi.org/10.2136/vzj2007.0074.

Šimůnek, J., Jarvis, N.J., Van Genuchten, M.T., Gärdenäs, A., 2003. Review and comparison of models for describing non-equilibrium and preferential flow and transport in the vadose zone. J. Hydrol. 272, 14–35.

Spanik, S., Rrokaj, E., Mondal, P.K., Sleep, B.E., 2021. Favorable and unfavorable attachment of colloids in a discrete sandstone fracture. J. Contam. Hydrol. 243, 103919.

Teshnizi, F.A., Ghobadinia, M., Abbasi, F., Hallett, P.D., Sepehrnia, N., 2023. Biochar and flow interruption control spatio-temporal dynamics of fecal coliform retention under subsurface drip irrigation. J. Contam. Hydrol. 253, 104128.

Torkzaban, S., Bradford, S.A., Walker, S., 2007. Colloid Retention in Variably Saturated Porous Media: Investigating the Effects of Hydrodynamic and Physiochemical Forces Using a Capillary Triangular Tube Model in the 2007 Annual Meeting.

Unc, A., Goss, M.J., 2003. Movement of faecal bacteria through the vadose zone. Water Air Soil Pollut. 149, 327–337.

Wang, X., Li, Y., Wang, Y., Liu, C., 2018. Performance of HYDRUS-1D for simulating water movement in water-repellent soils. Can. J. Soil Sci. 98, 407–420.

Wang, X., Li, Y., Chau, H.W., Tang, D., Chen, J., Bayad, M., 2021. Reduced root water uptake of summer maize grown in water-repellent soils simulated by HYDRUS-1D. Soil Tillage Res. 209, 104925.

Wang, J., Liao, J., Ma, J., Lyu, G., Yang, X., Ibekwe, A.M., Ma, J., 2023. Persistence of E. coli O157: H7 in frozen soils: role of freezing temperature. Sustainability 15, 13249.

Willmott, C.J., 1982. Some comments on the evaluation of model performance. Bull. Am. Meteorol. Soc. 63, 1309–1313.

Wolgemuth, C.W., 2008. Collective swimming and the dynamics of bacterial turbulence. Biophys. J. 95, 1564–1574.

Wu, H.Y., Jiang, D.H., Cai, P., Rong, X.M., Dai, K., Liang, W., Huang, Q.Y., 2011. Adsorption of Pseudomonas putida on soil particle size fractions: effects of solution chemistry and organic matter. J. Soils Sediments 12, 143–149.

Xu, S., Chen, X., Zhuang, J., 2019. Opposite influences of mineral-associated and dissolved organic matter on the transport of hydroxyapatite nanoparticles through soil and aggregates. Environ. Res. 171, 153–160.

Zhang, M., He, L., Jin, X., Bai, F., Tong, M., Ni, J., 2021. Flagella and their properties affect the transport and deposition behaviors of Escherichia coli in quartz sand. Environ. Sci. Technol. 55, 4964–4973.

Zheng, X., Bai, H., Tao, Y., Achak, M., Rossez, Y., Lamy, E., 2022. Flagellar phenotypes impact on bacterial transport and deposition behavior in porous media: case of salmonella enterica Serovar typhimurium. Int. J. Mol. Sci. 23, 14460.

Zhou, T., Levintal, E., Brunetti, G., Jordan, S., Harter, T., Kisekka, I., Šimůnek, J., Dahlke, H.E., 2023. Estimating the impact of vadose zone heterogeneity on agricultural managed aquifer recharge: a combined experimental and modeling study. Water Res. 247, 120781.